Environmental Science & Technology

Article

pubs.acs.org/est

Coupling between Chemical and Meteorological Processes under Persistent Cold-Air Pool Conditions: Evolution of Wintertime $PM_{2.5}$ Pollution Events and N_2O_5 Observations in Utah's Salt Lake Valley

Munkhbayar Baasandorj,[*,†,‡] Sebastian W. Hoch,[‡] Ryan Bares,[‡] John C. Lin,[‡] Steven S. Brown,[∥,⊥] Dylan B. Millet,[▽] Randal Martin,[○] Kerry Kelly,[§] Kyle J. Zarzana,[∥,#] C. David Whiteman,[‡] William P. Dube,[∥,#] Gail Tonnesen,[◆] Isabel Cristina Jaramillo,[§] and John Sohl[¶]

[†]Utah Department of Environmental Quality, Salt Lake City, Utah 84116, United States

[‡]Department of Atmospheric Sciences and [§]Department of Chemical Engineering, University of Utah, Salt Lake City, Utah 84112, United States

[∥]Chemical Sciences Division, Earth System Research Laboratory, National Oceanic and Atmospheric Administration, Boulder, Colorado 80305, United States

[⊥]Department of Chemistry and Biochemistry and [#]Cooperative Institute for Research in Environmental Sciences, University of Colorado, Boulder, Colorado 80309, United States

[▽]Department of Soil, Water, and Climate, University of Minnesota, St. Paul, Minnesota 55108, United States

[○]Civil and Environmental Engineering Department, Utah State University, Logan, Utah 84322, United States

[◆]Environmental Protection Agency Region VIII, Denver, Colorado 80202, United States

[¶]Department of Physics, Weber State University, Ogden, Utah 84408, United States

Supporting Information

ABSTRACT: The Salt Lake Valley experiences severe fine particulate matter pollution episodes in winter during persistent cold-air pools (PCAPs). We employ measurements throughout an entire winter from different elevations to examine the chemical and dynamical processes driving these episodes. Whereas primary pollutants such as NO_x and CO were enhanced twofold during PCAPs, O_3 concentrations were approximately threefold lower. Atmospheric composition varies strongly with altitude within a PCAP at night with lower NO_x and higher oxidants (O_3) and oxidized reactive nitrogen (N_2O_5) aloft. We present observations of N_2O_5 during PCAPs that provide evidence for its role in cold-pool nitrate formation. Our observations suggest that nighttime and early morning chemistry in the upper levels of a PCAP plays an important role in aerosol nitrate formation. Subsequent daytime mixing enhances surface $PM_{2.5}$ by dispersing the aerosol throughout the PCAP. As pollutants accumulate and deplete oxidants, nitrate chemistry becomes less active during the later stages of the pollution episodes. This leads to distinct stages of $PM_{2.5}$ pollution episodes, starting with a period of $PM_{2.5}$ buildup and followed by a period with plateauing concentrations. We discuss the implications of these findings for mitigation strategies.

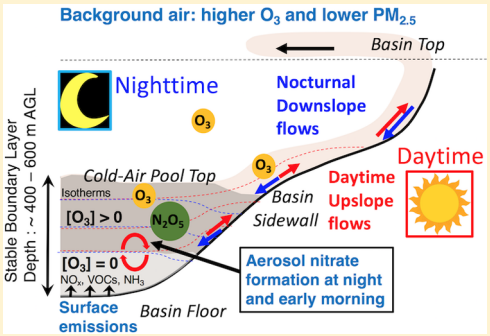

1. INTRODUCTION

The Salt Lake Valley (SLV), with a population of ~1 000 000, experiences elevated levels of particulate matter with aerodynamic diameter less than 2.5 μm ($PM_{2.5}$) in the winter months, with 24 h averaged values reaching up to 60−80 $\mu g\ m^{-3}$ (refs 1−4). These $PM_{2.5}$ pollution episodes are closely related to the passing of high-pressure ridges that favor the formation of persistent cold air pools (PCAPs) in Utah's topographic basins.[1,3,5] Under these conditions, the atmospheric boundary layer is stably stratified and/or confined by a capping inversion associated with warm air advection aloft. In a stably stratified atmosphere, mixing is limited, and pollutants emitted near the surface accumulate, leading to elevated levels of primary and secondary pollutants including $PM_{2.5}$. Despite large interannual variability in the number and intensity of PCAPs, a typical winter in the Salt Lake City Basin sees about six multiday PCAPs, comprising 18 days above the National Ambient Air Quality Standard (NAAQS) for the 24 h $PM_{2.5}$ of 35 $\mu g\ m^{-3}$ (refs 3,6,7). However, the fundamental chemical processes governing the formation of secondary aerosol in the SLV remain poorly understood. A better understanding of

Received: December 30, 2016
Revised: April 28, 2017
Accepted: May 3, 2017
Published: May 3, 2017

DOI: 10.1021/acs.est.6b06603
Environ. Sci. Technol. 2017, 51, 5941−5950

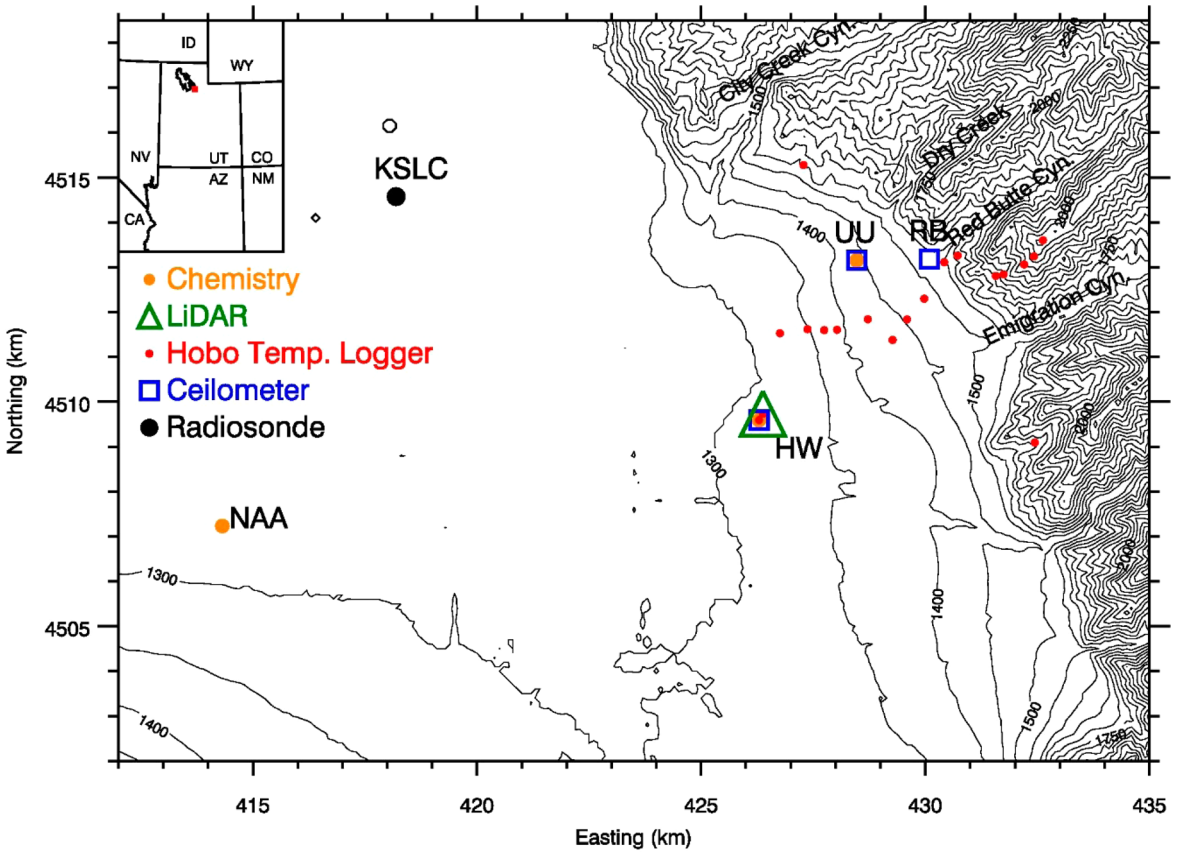

Figure 1. Topographic map (UTM zone 12 projection, 50 m elevation contours) of the northeastern part of the Salt Lake Valley, highlighting the locations of the main observational sites. Sites with extended observations of chemistry (orange dots), ceilometers (blue squares), a Doppler wind lidar (green triangle), and radiosonde launches (black circle) are shown. Automatic temperature dataloggers are shown in red.

these processes is crucial to enable prediction and to formulate effective control strategies.

The principal component of $PM_{2.5}$ in Utah valleys is ammonium nitrate (NH_4NO_3), which accounts for up to 70−80% of the total mass during the pollution episodes. In contrast, ammonium sulfate is a minor contributor.[8−15] Secondary ammonium chloride and organic aerosol can account for 10−15%[9] and up to 15−20% of total $PM_{2.5}$ mass,[6,10,15] respectively, on highly polluted days. Literature on the relative abundances, vertical and spatial variability, and sources of the aerosol precursors in the SLV is sparse although previous work indicates that NH_4NO_3 formation in this airshed is HNO_3 limited during winter $PM_{2.5}$ pollution episodes.[6,9]

NH_4NO_3 is formed in the atmosphere via a reversible reaction between gaseous ammonia (NH_3) and nitric acid (HNO_3).[16,17] NH_3 is emitted predominantly from agricultural sources, including animal husbandry and fertilizer applications. Other sources include automobile emissions, waste disposal and recycling, industrial processes, and volatilizations from soil and oceans.[18−20] In contrast, HNO_3 is formed in the atmosphere as a secondary oxidation product of NO_x. During the day, this conversion occurs primarily via:

$$OH + NO_2 \rightarrow HNO_3 \quad (1)$$

At night, the nocturnal chemistry of NO_3 and N_2O_5 leads to HNO_3 formation via:

$$NO_2 + O_3 \rightarrow NO_3 + O_2 \quad (2)$$

$$NO_3 + NO_2 + M \rightleftarrows N_2O_5 + M \quad (3)$$

$$N_2O_5 + H_2O_{(l)} \rightarrow 2HNO_3 \quad (4)$$

At colder temperatures, characteristic of the SLV in winter,[3] the equilibrium in reaction 3 shifts strongly to the left, favoring reactions of N_2O_5 over those of NO_3.[21,22] Reaction 4 is the most-important heterogeneous reaction globally for the removal of NO_x and formation of soluble inorganic nitrate.[21,23]

The heterogeneous uptake of N_2O_5 on chloride-containing particles can also release $ClNO_2$, a daytime chlorine radical precursor, which can influence morning radical chemistry.[24−26]

$$N_2O_5 + Cl^-(aq) \rightarrow ClNO_2 + NO_3^-(aq) \quad (5)$$

The relative contribution of daytime versus nighttime chemical pathways to HNO_3 formation during wintertime $PM_{2.5}$ pollution events in the SLV remains uncertain. Based on surface observations of HNO_3 and $PM_{2.5}$, Kuprov et al.[10] suggested that the daytime pathway was the most important. However, surface observations do not adequately characterize the chemical composition or processes occurring aloft. Due to the combination of inefficient mixing, particularly at night, and fresh emissions near the surface, the atmospheric composition and associated chemistry are expected to be highly altitude-dependent.[23,27−30] Under wintertime PCAP conditions characterized by low temperatures, limited solar insolation, fog and cloudiness, and high $PM_{2.5}$ mass loading,[3,31] HNO_3 production via N_2O_5 heterogeneous uptake could be a dominant process. Therefore, observations of NO_3, N_2O_5, and related species are essential to determine the role of nighttime chemistry and to establish when, where, and how HNO_3 and aerosol nitrate formation occurs.

DOI: 10.1021/acs.est.6b06603
Environ. Sci. Technol. 2017, 51, 5941−5950

Here, we present detailed chemical and meteorological observations in Salt Lake City, Utah from a moderately elevated site near the foothill of the Wasatch Mountains. This study aims to improve scientific understanding of the chemical and meteorological processes governing $PM_{2.5}$ pollution episodes. We compare the chemical and meteorological conditions at the surface and higher elevations by using a wide suite of surface observations from sites at different elevations. We then examine the processes important for the temporal evolution of $PM_{2.5}$ pollution, present the first observations of N_2O_5 in the SLV, and discuss the implications for mitigation.

2. METHODS

Measurements of a wide suite of chemical and meteorological parameters were made in the SLV from December 10, 2015 to February 28, 2016 as part of the wintertime $PM_{2.5}$ study. Figure 1 shows the locations and elevations of the observation sites. All trace gas and particulate measurements were made from the main site on the roof of the William Browning Building at the University of Utah (UU) at ~28 m AGL. The UU site is located along the northeast sidewall of SLV, roughly 155 m above the valley floor, away from major interstates and large industrial sources. The site is, however, impacted by local traffic and meteorological phenomena typical for basin sidewalls including diurnal, thermally driven circulations. Observations at UU included $PM_{2.5}$ mass concentrations, CO, O_3, NO_x (NO and NO_2), CO_2, CH_4, H_2O, N_2O_5, and NO_3, with analytical details provided in the Supporting Information. To contrast the chemical conditions on the valley floor and at higher elevations, we utilized near-surface NO_x, CO, and $PM_{2.5}$ data collected at two additional sites located on the valley floor: Hawthorne Elementary (HW) and Neil Armstrong Academy (NAA) (see the Supporting Information).

The supporting meteorological measurements investigated the formation, evolution and breakup of PCAPs. PCAPs were identified using the valley heat deficit (VHD),[3] a bulk thermodynamic measure of atmospheric static stability calculated based on twice-daily atmospheric sounding data. Previous research[3] has shown that daily NAAQS $PM_{2.5}$ exceedances are likely to follow when VHD first exceeds 4.04 MJ m^{-2}. VHD is calculated as

$$\mathrm{VHD} = c_p \int_{1288\ \mathrm{m}}^{2200\ \mathrm{m}} \rho(z)[\theta_{2200\ \mathrm{m}} - \theta(z)]\, dz \qquad (1a)$$

where 1288 and 2200 m are the valley floor and mean ridgeline elevations in the SLV, potential temperature $\theta(z)$ and air density $\rho(z)$ are obtained from radiosonde soundings, c_p is the specific heat of air at constant pressure, and dz is 10 m. 4.04 MJ m^{-2} is the climatological mean heat deficit for days when daily $PM_{2.5}$ concentrations exceeded half of the daily $PM_{2.5}$ NAAQS of 17.5 μg m^{-3}. Details of all meteorology observations, including vertical profiles of temperature and wind, aerosol backscatter from three ceilometer deployments, and near-surface turbulence parameters, are provided in the Supporting Information.

3. RESULTS AND DISCUSSION

3.1. Overview of This Study. Figure 2 gives an overview of key meteorological and chemical variables observed during this study. These include (Figure 2a) the observed hourly averaged $PM_{2.5}$ mass concentrations at UU (red) and HW (blue), the 24 h $PM_{2.5}$ levels (HW) relative to NAAQS for the 24 h $PM_{2.5}$ of

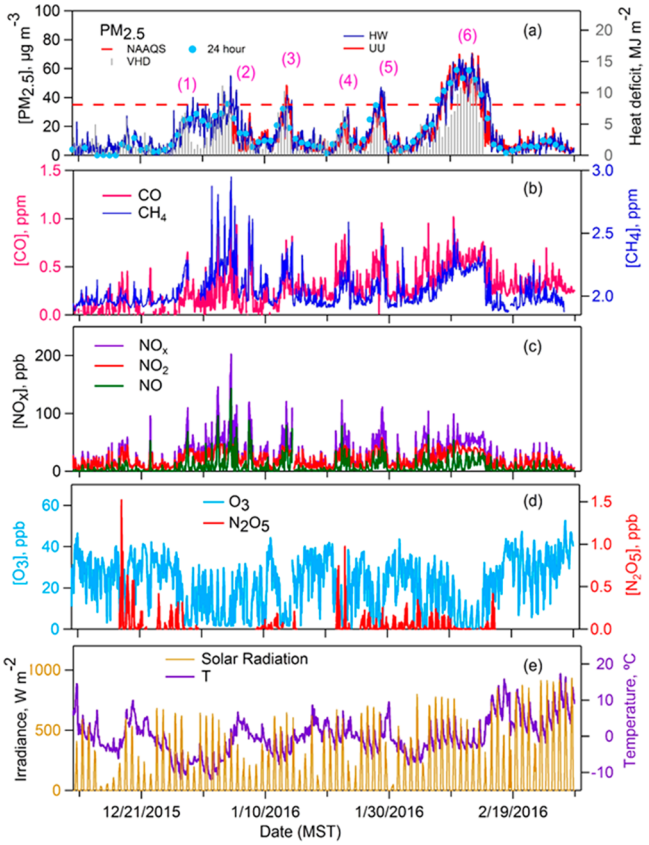

Figure 2. Time series of (a) 24 h and an hourly averaged $PM_{2.5}$ mass concentration at the UU and HW sites and valley heat deficit (b) mixing ratios of CO and CH_4; (c) mixing ratios of NO, NO_2, and NO_x; (d) O_3 and N_2O_5 mixing ratios; and (e) solar radiation and temperature measured at the UU site. The time series illustrates the episodic nature of enhancements in $PM_{2.5}$ and primary pollutants during PCAP events (1–6).

35 μg m^{-3} (blue circles versus dashed red line), and the twice-daily VHD (gray bars). Hourly averaged trace gas mixing ratios for CO, CH_4, NO_x, and O_3 and minute-averaged N_2O_5 mixing ratios are shown in Figure 2b–d. Hourly averaged incoming solar radiation and temperature recorded at UU are illustrated in Figure 2e. $PM_{2.5}$ concentrations measured at UU and HW (red and blue lines, Figure 2a) were nearly identical despite the different altitude of these sites. The homogeneity of $PM_{2.5}$ within the valley is one of the unique aspects of these wintertime pollution episodes, consistent with observations of Silcox et al.,[2] and has been observed in other mountain valleys.[32,33]

As shown in Figure 2a, $PM_{2.5}$ levels are highly episodic, with 24 h values varying from <2 to ~60 μg m^{-3} around a winter mean of 14.9 μg m^{-3}. A total of six multiday episodes with elevated $PM_{2.5}$ levels was observed during the 2015–2016 winter season, and they correspond to periods of strong atmospheric stability, as indicated by elevated VHD values.[3]

The 2015–2016 winter episodes are examined below and compared against episodes from past winter seasons to determine common patterns. Four of these pollution episodes (December 1–4, 2015; January 11–15, 21–24, and 26–29, 2016) were short-lived episodes with moderate $PM_{2.5}$ levels (24 h means: <35 μg m^{-3}) that lasted 4–5 days. The pollution episode of December 26 2015–January 5 2016 was a combination of two short PCAP episodes that were separated

DOI: 10.1021/acs.est.6b06603
Environ. Sci. Technol. 2017, 51, 5941–5950

by a 3 day hiatus when the VHD remained below the threshold value[3] of 4.04 MJ m^{-2}. The February 6−16, 2016 pollution episode was the longest-lived pollution episode of the season, with the highest $PM_{2.5}$ values and eight consecutive daily exceedances. This episode is examined in detail in section 3.4.

The overview of trace gas observations (Figure 2b−d) shows that CO, CH_4, and NO_x were elevated during PCAP episodes, reaching up to 1.2 ppm, 3 ppm, and 200 ppb, respectively, at UU (Figure 2b,c). However, the daily maximum O_3 was ∼10−45 ppb, with lower levels during the pollution episodes (Figure 2d). N_2O_5 was detectable at UU on most nights (Figure 2d). Nighttime O_3 and N_2O_5 were nonzero at this site during clean periods and even at times during the pollution episodes. The highest observed N_2O_5 mixing ratios were 0.3 and 1.52 ppb during and outside pollution periods, respectively, with an average nocturnal value of 0.076 ppb for the study period.

3.2. Spatiotemporal Variation of Pollutant Concentrations. Figure 3 shows the mean diurnal cycles of hourly averaged concentrations of (a) NO, (b) O_3, and (c) $PM_{2.5}$ measured at UU, HW, and NAA to illustrate the differences in chemical conditions at the valley floor (HW and NAA) versus higher elevations on the valley sidewall (UU). At HW, NO concentrations are on average 2 and 4 times greater than the levels seen at NAA and UU, respectively, and exhibit a morning peak reaching up to 55 ppb at ∼8 AM when this site is impacted by fresh emissions from nearby roads and highways. The morning NO peak at UU is ∼3 times lower than the peak at HW and lags HW by 1 h. This time lag likely reflects the transport and mixing of pollutants from the center of the valley toward the valley sidewall. Daytime O_3 levels are comparable at the three sites with a peak concentration of ∼30 ppb (Figure 3b). However, considerable variation in O_3 is seen during nighttime, with the highest O_3 observed at UU. This indicates that while O_3 is titrated on the valley floor at night due to the presence of high NO_x, it is still present at higher elevation sites with lower NO_x, allowing nighttime chemistry through reactions 2−4 to take place. Compared to differences in O_3 and NO_x, $PM_{2.5}$ mass concentrations exhibit less variability across different sites. This homogeneity in $PM_{2.5}$ is consistent with conversion of gas-phase precursors to secondary aerosol and a lifetime of $PM_{2.5}$ on the order of several days, long enough to allow for the dispersion of $PM_{2.5}$ across the basin.

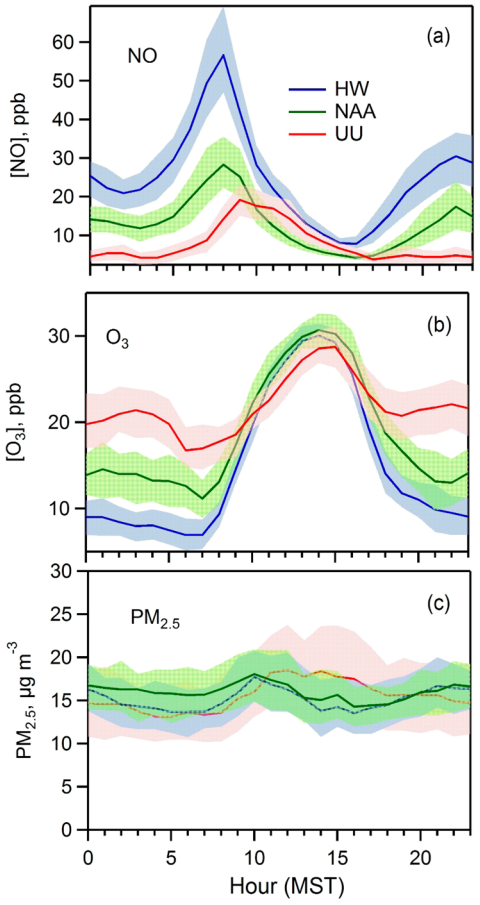

Figure 3. Diurnal variation of (a) NO and (b) O_3 mixing ratios and (c) $PM_{2.5}$ mass concentrations at HW, NAA, and UU sites during this study. The NO_x and O_3 levels show a considerable variation from site to site with lowest NO_x and highest O_3 observed at the UU site. In contract, $PM_{2.5}$ levels are relatively homogeneous across the valley.

Chemical and meteorological conditions during and outside pollution episodes are discussed in detail in the Supporting Information. During pollution episodes, the basin atmosphere as a whole remains stably stratified throughout the day, and pollutants remain trapped; however, the lower portion of the PCAP becomes statically unstable during the day (Figure S1). Our observations indicate slower transport of pollutants across the valley during pollution episodes due to more stagnant conditions with low wind speeds and high atmospheric stability. Pollution episodes are characterized by higher NO_x concentrations, higher relative humidity, colder temperatures, and lower O_3 concentrations (Figure S2). Enhancements of up to factor of 4 in NO_x and lower O_3 with a daily maxima of ∼20 ppb and an average nighttime value of ∼7 ppb are observed at UU during pollution episodes. Unlike NO_x, O_x (NO_2 + O_3) exhibits less variation with a modest enhancement in the afternoon during pollution episodes. The weak O_x enhancement seen in the afternoon could be a measure of local photochemistry.

3.3. Stages of $PM_{2.5}$ Episodes: $PM_{2.5}$ Buildup and Plateau Period. A comparison of the longest-lived episode of winter 2015−2016 with major episodes of past winters shows that there are features common to all major episodes that have occurred in the SLV since 1999. We examine two major episodes from past winters in Figure 4 because extended pollution episodes provide the best illustration of the distinct stages of the meteorological and chemical evolution. These stages include a period of $PM_{2.5}$ buildup, a period of high but plateauing $PM_{2.5}$ concentrations, and a PCAP breakup period with decreasing $PM_{2.5}$ concentrations (Figure 4a). The initial stage is characterized by a period with a steady increase in $PM_{2.5}$ and frequently cloud-free conditions. $PM_{2.5}$ levels first rise to ∼60 $\mu g\ m^{-3}$ over 5−7 days at a rate of 6−10 $\mu g\ m^{-3}\ day^{-1}$ (refs 2 and 3). If the PCAP conditions persist, the next stage is a period of plateauing $PM_{2.5}$ that frequently coincides with a fog-filled or cloud-topped PCAP. As shown in Figure 4a, the VHD (gray bars) remained above the threshold value of 4.04 MJ m^{-2} during the January 2004 episode. The threshold for 24 h $PM_{2.5}$ appears to be approximately 60 $\mu g\ m^{-3}$ in the SLV as the daily mass concentrations rarely exceed this level. This observation is consistent with the climatological analysis conducted by Whiteman et al.[3] However, if a short interruption in PCAP conditions occurs during the later stage of a pollution episode, as in December 2001, it drives $PM_{2.5}$ enhancements above the typical threshold (Figure 4b), as discussed in section 3.5.

DOI: 10.1021/acs.est.6b06603
Environ. Sci. Technol. 2017, 51, 5941−5950

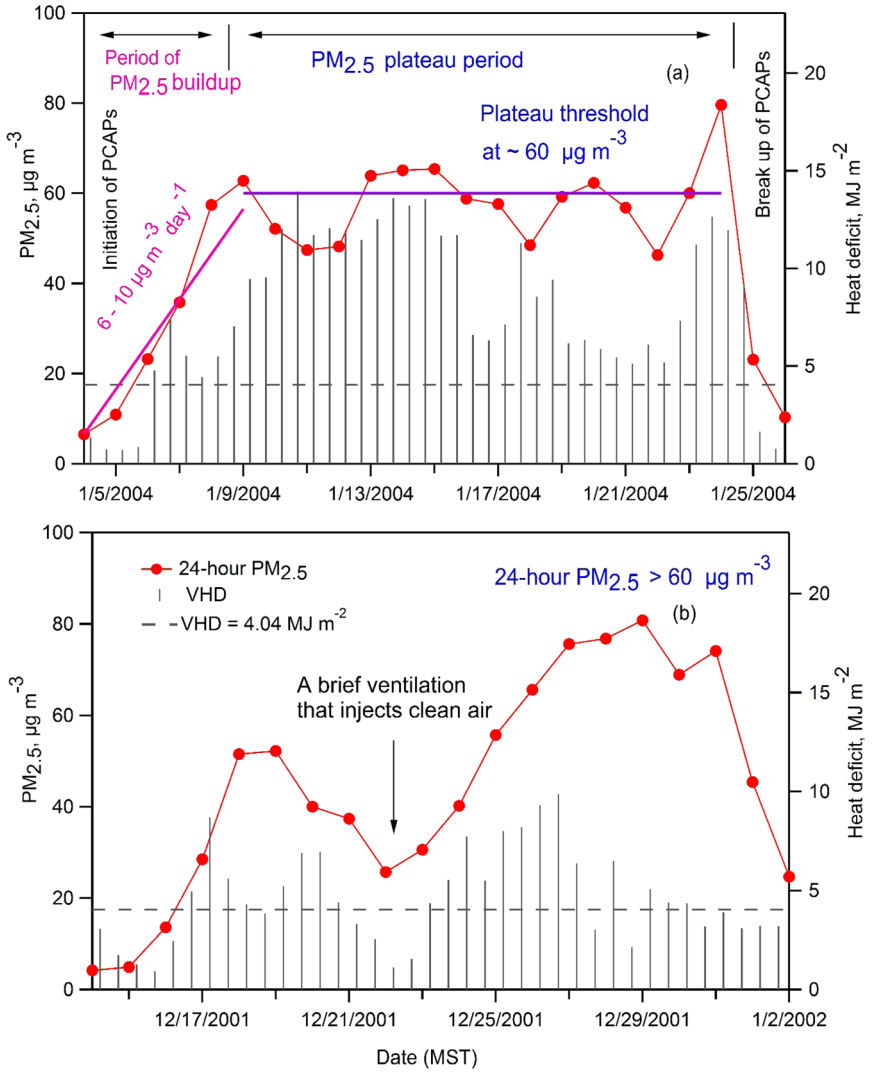

Figure 4. (a) Time evolution of $PM_{2.5}$ pollution during a long-lasting episode. It shows the distinct stages of $PM_{2.5}$ pollution episodes that consist of periods of buildup followed by a plateau of $PM_{2.5}$ at a threshold value of ~60 μg m^{-3}. (b) An example long-lived episode with 24 h $PM_{2.5}$ levels exceeding the threshold of 60 μg m^{-3}. During this episode, an interruption in atmospheric stability led to a brief ventilation, which gave rise to a buildup of elevated 24 h $PM_{2.5}$ levels above the typical threshold.

3.4. Case Study: February 6–16, 2016 Episode. Chemical and meteorological conditions during this pollution episode are examined in Figures 5, 6, and S3. NO_x accumulates, reaching values as high as ~200 and ~100 ppb at HW and UU, respectively, and eventually converging at both sites. This convergence is indicative of a valley-wide buildup of NO_x, particularly during the later stages of the pollution episode (Figure 5b). Peak O_3 and N_2O_5 concentrations and production of nitrate radicals (P_{NO_3}) (see eq 2a below) exhibit an opposite trend decreasing over time (Figure 5c,d) consistent with oxidant titration by excess NO:

$$NO + O_3 \rightarrow NO_2 + O_2 \quad (6)$$

O_3 is completely titrated at night at HW, which is rich in NO_x, consistent with a near-surface layer with excess NO_x that is devoid of oxidants. In contrast, at the higher elevation UU site, O_3 levels as high as 20 ppb are still present at night during the $PM_{2.5}$ buildup period, indicating favorable conditions for HNO_3 formation. However, O_3 becomes depleted at the higher elevation after day 5–6, which suggests spreading of the oxidant limited condition to higher elevations.

The production rate of NO_3 radicals via reaction 2, P_{NO_3}, is shown in Figure 5d:

$$P_{NO_3} = k_2[O_3][NO_2] \quad (2a)$$

P_{NO_3} as measured at surface level during daytime does not lead to N_2O_5 or soluble nitrate production due to NO_3 photolysis and reaction with NO. However, if the surface level composition during late afternoon is representative of the mixed pollution layer in the convective boundary layer (CBL), then late afternoon surface-level P_{NO_3} will approximately reflect nighttime P_{NO_3} aloft. Accumulation of NO_x within a newly formed shallow nocturnal boundary layer leads to the observed, rapid O_3 titration and limited nighttime chemistry, even though nighttime chemistry may be active in the remainder of the PCAP aloft. Figure 5d shows that late afternoon P_{NO_3} is on the order of 2 ppb hr^{-1} at the onset of the pollution episode but decreases to 0.5 ppb hr^{-1} later in the event. Thus, there is a potential for significant nighttime production of aerosol nitrate in the elevated levels of the PCAP through nighttime N_2O_5

DOI: 10.1021/acs.est.6b06603
Environ. Sci. Technol. 2017, 51, 5941–5950

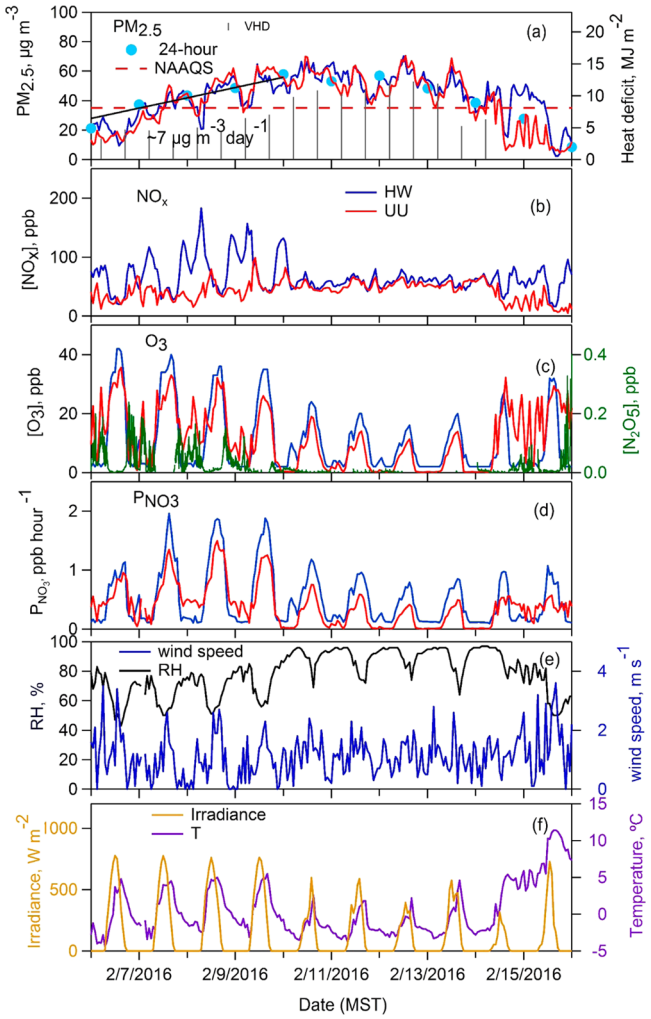

Figure 5. Time series of (a) hourly and 24 h mean $PM_{2.5}$ and VHD, (b) NO_x, (c) O_3 and N_2O_5 mixing ratios, (d) calculated P_{NO_3}, (e) wind speed and RH, and (f) incoming solar radiation and T observed during the February 6−16 episode. After a period of initial $PM_{2.5}$ buildup, which is characterized by rising $PM_{2.5}$ and NO_x levels with moderate levels of O_3 and N_2O_5 present at night at higher elevations, the nitrate formation appears to slow down at later stages of the pollution episode as the aerosol layer becomes oxidant deprived.

production. This potential decreases over time due to the observed decrease in P_{NO_3}. Observed N_2O_5 mixing ratios decreased from ∼200 ppt at the beginning to levels below the instrumental detection limit of 8 ppt (3σ, 1 s) later in the pollution episode (Figure 5c). The temporal evolution of the vertical profiles of T and RH during the episode and their effect on NH_4NO_3 dissociation constant (K_p) and phase transitions are discussed in Figure S3. Our observations indicate interesting time and altitude-dependent features of K_p and equilibrium state during PCAPs.

3.4.1. $PM_{2.5}$ Buildup Period. This period is characterized by lower NO_x and higher O_3 and N_2O_5 concentrations in the upper pollution layer at night. Figure 6 illustrates the time-height cross section of aerosol back scatter (β) recorded at HW and the corresponding surface observations of $PM_{2.5}$ concentrations, N_2O_5, NO_x, and O_3 mixing ratios at HW and UU during the $PM_{2.5}$ buildup period. During these 3 days, β shows a trend to higher values, corresponding to a general increase in $PM_{2.5}$ concentrations. Besides the general trend reflecting the buildup of pollution, a diurnal evolution pattern is revealed that reflects both meteorological and chemical processes. Increases in back scatter in the lower part of the basin atmosphere are typically seen during nighttime and in the early morning hours immediately after sunrise. RH increased over time but remained below the deliquescence RH (DRH) of NH_4NO_3 and exhibited less vertical variation at the early stage of the pollution episode (see Figure S3d). This indicates a minor role of hygroscopic growth of NH_4NO_3 on β during this period. Also, due to stable conditions as indicated by the weak winds aloft (arrows in Figure 6) and near the surface at night, the effect of transport on β is expected to be small. Hence, we attribute the increase in β to enhancements in aerosol concentration through condensation of ammonium nitrate at night and early morning. During these nights, N_2O_5 levels up to ∼200 ppt were observed between ∼1700 and ∼0800 MST the next morning, providing evidence for aerosol nitrate formation via reactions 2−4. Early morning increases in the aerosol back scatter observed at ∼8−10 AM MST reflect a brief period of active chemistry leading to an increase in aerosol concentrations up to 200 m AGL following sunrise.

The development of a surface-based CBL and daytime mixing of aerosols to elevated layers within the PCAP is indicated by a deepening of elevated β values through the afternoon hours (Figure 6). This mixing process, also indicated in the pseudovertical temperature profiles measured along the basin sidewall (Figure S1), reaching levels of ∼400 m AGL is further corroborated by surface observations of turbulence kinetic energy and in lidar observations of the vertical wind velocity variance (not shown). Corresponding surface observations exhibit a rapid increase in $PM_{2.5}$ and a decrease in NO_x (Figures 6 and S2a,c) consistent with the transport of aerosol-rich, low-NO_x air from aloft to the surface. Surface aerosol composition measurements at NAA lend further support as NH_4NO_3 accounted for the majority of the $PM_{2.5}$ (∼73%) during this episode in accordance with previous studies and showed a day-to-day enhancement consistent with the observed $PM_{2.5}$ buildup. Surface-based mixing continues until sunset, setting up the potential for nighttime chemistry in the upper levels of the PCAP during the following night.

A similar pattern can be seen in aerosol back scatter profiles and the diurnal changes of $PM_{2.5}$, CO, and NO_x during 2015−2016 winter and past winter episodes. This coupling between the chemistry and transport is similar to $PM_{2.5}$ characteristics observed in other valleys[33−39] and the Great Lakes Region[40,41] during winter. Enhanced NH_4NO_3 layers have also been observed outside the winter season within nocturnal boundary layers (at ∼100 m AGL)[29,30] and at higher altitudes.[42,43] Through vertical mixing, NH_4NO_3-rich upper layers can contribute to the particulate matter near the ground,[42] as observed in SLV. However, NH_4NO_3 enhancements observed at higher altitudes in warmer seasons are mostly driven by a negative temperature gradient and the positive gradient in RH with altitude.[42,43] In contrast, chemical factors and the vertical distributions of the precursor gases appear to be the main drivers of the vertical characteristics of cold pool NH_4NO_3. Using tethered balloon measurements, Ferrero et al.[35−37] studied the aerosol accumulation over Italian valleys within the mixing layer under stagnation conditions and reported that the relative contribution of the fine fraction enriched in secondary inorganic ions increased with altitude within the mixing height and above, which was attributed to the aerosol aging due to coagulation and condensation.[35,36] Measurements at the surface

DOI: 10.1021/acs.est.6b06603
Environ. Sci. Technol. 2017, 51, 5941−5950

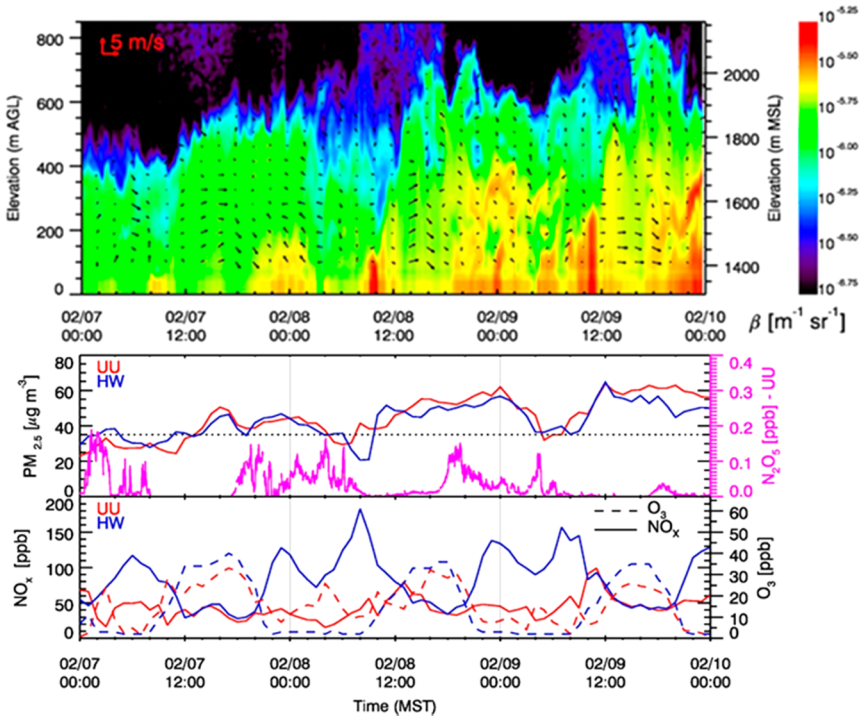

Figure 6. Time−height cross-section of aerosol back scatter coefficient β (color contours) at HW during the initial 3 days of the buildup period of the February 6−16, 2016 pollution episode. The wind lidar retrieved vertical profile of horizontal winds is shown as vectors. Bottom panels show corresponding HW (blue) and UU (red) surface $PM_{2.5}$, NO_x, and O_3. N_2O_5 concentrations at UU are shown in pink. The increase in β around midnight and 8−11 AM MST indicate an aerosol nitrate formation that takes place at night and early in the morning in the upper layer. A subsequent mixing within a surface-based CBL disperses and transports the aerosol-rich air to the top of the aerosol layer and down to the surface, leading to the enhancements in surface $PM_{2.5}$ levels and the decrease in surface NO_x between 11 and 12 MST.

and on a tower (90 m) in San Joaquin Valley during a $PM_{2.5}$ episode show similar vertical features of O_3 and NO_x as observed in the SLV and increases in accumulation-mode particles and nitrate concentrations aloft during the nighttime and early morning, consistent with an aloft nighttime nitrate formation mechanism.[34] In accordance with the chemistry and transport features observed in the SLV, CMAQ modeling of wintertime NH_4NO_3 in the Great Lakes Region predicts a substantial vertical gradient in nitrate partitioning with concentrations of HNO_3 and N_2O_5 and NO_3^- formation maxima aloft (100−500 m) and estimates that the nighttime HNO_3 formation pathways can account for 72% of the total nitrate production in winter.[40,41] To the best of our knowledge, observations of N_2O_5 in the SLV represent the first N_2O_5 measurements under PCAPs conditions and provide evidence for the importance of nighttime pathways in cold-pool nitrate formation.

3.4.2. $PM_{2.5}$ Plateau Period. This period is characterized by excess NO_x, oxidant depleted conditions, low temperatures, and high (~100%) RH above the DRH in the lower portion of the PCAPs (Figure S3e,f). Figure 5c,d shows reduced O_3 and P_{NO_3} during this stage of the episode, indicating a reduced rate of NO_x oxidation and, thus, NO_3^- production. If the rate of NO_3^- production becomes slow enough to be balanced by aerosol loss processes such as deposition, increased dissociation of NH_4NO_3 at the top of the PCAP as indicated by the enhancement in the *K*p (Figure S3b,c) or transport out of the PCAP, then the observed lack of further increases in $PM_{2.5}$ would represent an approximate steady state. Further evidence for this hypothesis is presented below in section 3.5, together with suggestions for further observational tests. Meteorological effects, such as the transition to a cloud-topped PCAP and a change from daytime surface-based mixing processes to mixing processes due to cloud-top cooling may also play a role in diluting the pollutants during this period.

3.5. Potential Oxidant Sources and the Role of Oxidant Injections. Photochemical generation of free radicals is weak during wintertime due to reduced solar insolation, low ozone, and low absolute water vapor concentrations that combine to significantly reduce OH radical generation from ozone photolysis.[44] Potential radical sources that may drive early morning chemistry are photolabile nighttime radical reservoirs, such as $ClNO_2$ and HONO, which are known to form and accumulate overnight and photolyze in the morning.[23,45] Given the presence of aerosol chloride in the SLV[9] and the evidence of N_2O_5 chemistry at night, chlorine activation via reaction 5 could be an important radical source. Morning $ClNO_2$ photolysis leads to production of Cl + NO_2. The Cl radical will most likely propagate through reaction of hydrocarbons and subsequent peroxy radical cycling to produce additional HO_x radicals. In the high-NO_x conditions of a PCAP, these HO_x radicals will then further increase the oxidation of NO_2 to NO_3^-, leading to an additional, morning source of NH_4NO_3. The amount of this morning production depends on the chain length of radical propagation and is beyond the scope of this manuscript to quantitatively predict. However, $ClNO_2$ activation has the potential to increase soluble nitrate formation beyond what would occur from nighttime chemistry alone. Photolysis of carbonyl compounds may also be important for daytime radical generation in the SLV, especially if there are significant direct emissions of formaldehyde from mobile and other urban and residential wood combustion sources.[46]

DOI: 10.1021/acs.est.6b06603
Environ. Sci. Technol. 2017, 51, 5941−5950

An alternative source of oxidants is the injection of background air from outside the PCAP, often seen in the aerosol back scatter profiles. Possible processes are nocturnal down-valley circulations in the tributary canyons, the lake breeze from the Great Salt Lake, or ventilation of the pollution layer due to a partial mix-out of the cold-air pool associated with a synoptic disturbance. Tropospheric background O_3 mixing ratios in Utah in winter are typically 30−50 ppb,[47] and thus, the background air is enriched in O_3 compared to the oxidant limited air within the PCAP. Hence, the influx of background air into an oxidant limited photochemical regime can supply oxidants that fuel the nitrate formation while diluting the pollutants, thereby having competing effects on $PM_{2.5}$ concentrations.

Since 1999, there have been only a handful of episodes during which 24 h $PM_{2.5}$ levels exceeded the plateau threshold of ∼60 $\mu g\ m^{-3}$. These episodes were influenced by factors such as injection of cleaner air due to a partial mix-out. Figure 4b shows an example of such an episode, with $PM_{2.5}$ levels reaching up to ∼80 $\mu g\ m^{-3}$. The VHD (gray bars) dipped below the PCAP threshold value of 4.04 MJ m^{-2} on day 7−8, indicating a brief ventilation or partial mix-out. As shown, the influx of the background air led to an initial drop in $PM_{2.5}$ followed by an increase in $PM_{2.5}$ levels above the typical $PM_{2.5}$ plateau threshold. If oxidant limitation in the conversion of NO_x to nitrate is the explanation for the apparent steady state observed during other PCAP events, and if mixing with O_3 rich air from above the PCAP is a significant oxidant source, then the evolution of $PM_{2.5}$ to higher levels during this event is consistent with mixing of O_3 rich air providing a source of oxidant. However, testing this hypothesis requires further observations of vertical profiles of NO_x, O_3, and other trace gases, together with atmospheric chemical modeling.

3.6. Implications. Our observations indicate that active nighttime and early morning chemistry leads to aerosol nitrate formation in the upper part of the PCAPs during pollution episodes. Subsequent mixing of aerosol-rich air from upper layers to the surface during the day likely contributes to the observed midmorning surface $PM_{2.5}$ maxima. However, over time, the system becomes NO_x saturated as the PCAP persists, quenching the oxidants for both nighttime chemistry and photochemistry within the pollution layer. If the system is indeed oxidant limited, and if NO_x emissions primarily have the effect of removing oxidants, then control strategies based on NO_x reduction could perturb the observed $PM_{2.5}$ plateau typical of most PCAPs in the SLV, indicating a nonlinear response of this system to changes in precursor concentrations.

Because of the complex coupling between chemistry and transport, attribution of the limiting reagent for the NH_4NO_3 formation is difficult. NH_4NO_3 formation is likely limited by the availability of HNO_3 in the SLV based on the sensitivity of $PM_{2.5}$ to oxidant availability and the timing of $PM_{2.5}$ enhancements. However, it is possible that different regimes are present as a function of altitude and time during the pollution episodes, especially if there is a strong vertical gradient in NH_3. As pollution builds up in a PCAP, the system appears to turn into a more HNO_3-limited regime. However, NH_3 could potentially be the limiting reagent at higher elevation during the initial $PM_{2.5}$ buildup period in areas such as the SLV, where the system is close to the transition between NH_3- and HNO_3-limited regimes.[10] More information on the relative abundances of total nitrate and ammonium in the upper layers is needed to determine which precursor limits NH_4NO_3 formation and to what extent. Detailed vertically resolved measurements of gas and aerosol species involved in NH_4NO_3 formation would help to constrain chemical pathways and thermodynamic equilibrium.

■ ASSOCIATED CONTENT

Supporting Information

The Supporting Information is available free of charge on the ACS Publications website at DOI: 10.1021/acs.est.6b06603.

Figures showing a subset of temperature profiles, mean diurnal variation, and vertical profiles of T and K_p. Additional details on sites and observations and supplementary analyses. (PDF)

■ AUTHOR INFORMATION

Corresponding Author

*E-mail: m.baasandorj@utah.edu.

ORCID

Munkhbayar Baasandorj: 0000-0003-2320-8333

Kyle J. Zarzana: 0000-0003-1581-6419

Notes

The authors declare no competing financial interest.

■ ACKNOWLEDGMENTS

The wintertime $PM_{2.5}$ study was supported by the Utah Division of Air Quality. Additional funding came from the United States Environmental Protection Agency's Community Scale Air Toxics grant no. 96834601 (M.B.), from the Office of Naval Research award no. N00014-11-1-0709 (S.W.H. and C.D.W.), and from NSF grant no. 1723337 (S.W.H.).

■ REFERENCES

(1) Lareau, N. P.; Crosman, E.; Whiteman, C. D.; Horel, J. D.; Hoch, S. W.; Brown, W. O. J.; Horst, T. W. The Persistent Cold-Air Pool Study. *Bull. Am. Meteorol. Soc.* **2013**, *94* (1), 51.

(2) Silcox, G. D.; Kelly, K. E.; Crosman, E. T.; Whiteman, C. D.; Allen, B. L. Wintertime $PM_{2.5}$ concentrations during persistent, multi-day cold-air pools in a mountain valley. *Atmos. Environ.* **2011**, *46*, 17−24.

(3) Whiteman, C. D.; Hoch, S. W.; Horel, J. D.; Charland, A. Relationship between particulate air pollution and meteorological variables in Utah's Salt Lake Valley. *Atmos. Environ.* **2014**, *94*, 742−753.

(4) United States Environmental Protection Agency. *Air Quality System Data Mart.* https://www.epa.gov/airdata (accessed May 9, 2017).

(5) Green, M. C.; Chow, J. C.; Watson, J. G.; Dick, K.; Inouye, D. Effects of snow cover and atmospheric stability on winter $PM_{2.5}$ concentrations in Western U.S. valleys. *J. Appl. Meteor. Climatol.* **2015**, *54* (6), 1191−1201.

(6) Utah Division of Air Quality. *Utah State Implementation: Plan Control Measures for Area and Point Sources, Fine Particulate Matter, $PM_{2.5}$ SIP for the Salt Lake City, UT Nonattainment Area.* http://www.deq.utah.gov/Laws_Rules/daq/sip/docs/2014/12Dec/SIP%20IX.A.21_SLC_FINAL_Adopted%2012-3-14.pdf (assessed May 9, 2017).

(7) United States Environmental Protection Agency. *National Ambient Air Quality Standards for Particulate Matter; Final Rule; 40 CFR Part 50.* https://www.gpo.gov/fdsys/pkg/FR-2006-10-17/pdf/06-8477.pdf (assessed May 9, 2017).

(8) Hansen, J. C.; Woolwine, W. R.; Bates, B. L.; Clark, J. M.; Kuprov, R. Y.; Mukherjee, P.; Murray, J. A.; Simmons, M. A.; Waite, M. F.; Eatough, N. L.; Eatough, D. J.; Long, R.; Grover, B. D. Semicontinuous $PM_{2.5}$ and PM_{10} mass and composition measurements

DOI: 10.1021/acs.est.6b06603
Environ. Sci. Technol. 2017, 51, 5941−5950

in Lindon, Utah, during winter 2007. *J. Air Waste Manage. Assoc.* **2010**, *60* (3), 346−355.
(9) Kelly, K. E.; Kotchenruther, R.; Kuprov, R.; Silcox, G. D. Receptor model source attributions for Utah's Salt Lake City airshed and the impacts of wintertime secondary ammonium nitrate and ammonium chloride aerosol. *J. Air Waste Manage. Assoc.* **2013**, *63* (5), 575−590.
(10) Kuprov, R.; Eatough, D. J.; Cruickshank, T.; Olson, N.; Cropper, P. M.; Hansen, J. C. Composition and secondary formation of fine particulate matter in the Salt Lake Valley: Winter 2009. *J. Air Waste Manage. Assoc.* **2014**, *64* (8), 957−969.
(11) Long, R. W.; Eatough, N. L.; Mangelson, N. F.; Thompson, W.; Fiet, K.; Smith, S.; Smith, R.; Eatough, D. J.; Pope, C. A.; Wilson, W. E. The measurement of $PM_{2.5}$, including semi-volatile components, in the EMPACT program: results from the Salt Lake City Study. *Atmos. Environ.* **2003**, *37* (31), 4407−4417.
(12) Long, R. W.; Eatough, N. L.; Eatough, D. J.; Meyer, M. B.; Wilson, W. E. Continuous determination of fine particulate matter mass in the Salt Lake City Environmental Monitoring Project: A comparison of real-time and conventional TEOM monitor results. *J. Air Waste Manage. Assoc.* **2005**, *55* (12), 1782−1796.
(13) Long, R. W.; Modey, W. K.; Smith, P. S.; Smith, R.; Merrill, C.; Pratt, J.; Stubbs, A.; Eatough, N. L.; Eatough, D. J.; Malm, W. C.; Wilson, W. E. One− and Three−Hour $PM_{2.5}$ characterization, speciation, and source apportionment using continuous and integrated samplers. *Aerosol Sci. Technol.* **2005**, *39* (3), 238−248.
(14) Mangelson, N. F.; Lewis, L.; Joseph, J. M.; Cui, W. X.; Machir, J.; Eatough, D. J.; Rees, L. B.; Wilkerson, T.; Jensen, D. T. The contribution of sulfate and nitrate to atmospheric fine particles during winter inversion fogs in Cache Valley, Utah. *J. Air Waste Manage. Assoc.* **1997**, *47* (2), 167−175.
(15) Silva, P. J.; Vawdrey, E. L.; Corbett, M.; Erupe, M. Fine particle concentrations and composition during wintertime inversions in Logan, Utah, USA. *Atmos. Environ.* **2007**, *41* (26), 5410−5422.
(16) Stelson, A. W.; Seinfeld, J. H. Relative humidity and temperature dependence of the ammonium nitrate dissociation constant. *Atmos. Environ.* **1982**, *16* (5), 983−992.
(17) Mozurkewich, M. The dissociation constant of ammonium nitrate and its dependence on temperature, relative humidity and particle size. *Atmos. Environ., Part A* **1993**, *27* (2), 261−270.
(18) Perrino, C.; Catrambone, M.; Di Menno Di Bucchianico, A.; Allegrini, I. Gaseous ammonia in the urban area of Rome, Italy and its relationship with traffic emissions. *Atmos. Environ.* **2002**, *36* (34), 5385−5394.
(19) Behera, S. N.; Sharma, M.; Aneja, V. P.; Balasubramanian, R. Ammonia in the atmosphere: a review on emission sources, atmospheric chemistry and deposition on terrestrial bodies. *Environ. Sci. Pollut. Res.* **2013**, *20* (11), 8092−8131.
(20) Livingston, C.; Rieger, P.; Winer, A. Ammonia emissions from a representative in-use fleet of light and medium-duty vehicles in the California South Coast Air Basin. *Atmos. Environ.* **2009**, *43* (21), 3326−3333.
(21) Chang, W.; Bhave, P.; Brown, S.; Riemer, N.; Stutz, J.; Dabdub, D. Heterogeneous atmospheric chemistry, ambient measurements, and model calculations of N_2O_5: A review. *Aerosol Sci. Technol.* **2011**, *45* (6), 665−695.
(22) Wagner, N. L.; Riedel, T. P.; Young, C. J.; Bahreini, R.; Brock, C. A.; Dubé, W. P.; Kim, S.; Middlebrook, A. M.; Öztürk, F.; Roberts, J. M.; Russo, R.; Sive, B.; Swarthout, R.; Thornton, J. A.; VandenBoer, T. C.; Zhou, Y.; Brown, S. S. N_2O_5 uptake coefficients and nocturnal NO_2 removal rates determined from ambient wintertime measurements. *J. Geophys. Res.: Atmos.* **2013**, *118* (16), 9331−9350.
(23) Brown, S. S.; Stutz, J. Nighttime radical observations and chemistry. *Chem. Soc. Rev.* **2012**, *41* (19), 6405−6447.
(24) Finlayson-Pitts, B. J.; Ezell, M. J.; Pitts, J. N., Jr. Formation of chemically active chlorine compounds by reactions of atmospheric NaCl particles with gaseous N_2O_5 and $ClONO_2$. *Nature* **1989**, *337* (6204), 241.
(25) Osthoff, H. D.; Roberts, J. M.; Ravishankara, A. R.; Williams, E. J.; Lerner, B. M.; Sommariva, R.; Bates, T. S.; Coffman, D.; Quinn, P. K.; Dibb, J. E.; Stark, H.; Burkholder, J. B.; Talukdar, R. K.; Meagher, J.; Fehsenfeld, F. C.; Brown, S. S. High levels of nitryl chloride in the polluted subtropical marine boundary layer. *Nat. Geosci.* **2008**, *1* (5), 324−328.
(26) Thornton, J. A.; Kercher, J. P.; Riedel, T. P.; Wagner, N. L.; Cozic, J.; Holloway, J. S.; Dubé, W. P.; Wolfe, G. M.; Quinn, P. K.; Middlebrook, A. M.; Alexander, B.; Brown, S. S. A large atomic chlorine source inferred from mid- continental reactive nitrogen chemistry. *Nature* **2010**, *464* (7286), 271.
(27) Brown, S. S.; Dubé, W. P.; Osthoff, H. D.; Wolfe, D. E.; Angevine, W. M.; Ravishankara, A. R. High resolution vertical distributions of NO_3 and N_2O_5 through the nocturnal boundary layer. *Atmos. Chem. Phys.* **2007**, *7* (1), 139−149.
(28) Stutz, J.; Alicke, B.; Ackermann, R.; Geyer, A.; White, A.; Williams, E., Vertical profiles of NO_3, N_2O_5, O_3, and NO_x in the nocturnal boundary layer: 1. Observations during the Texas Air Quality Study 2000. *J. Geophys. Res.* **2004**, *109* (D12); 10.1029/2003JD004209.
(29) Rinaldi, M.; Gilardoni, S.; Paglione, M.; Sandrini, S.; Fuzzi, S.; Massoli, P.; Bonasoni, P.; Cristofanelli, P.; Marinoni, A.; Poluzzi, V.; Decesari, S. Organic aerosol evolution and transport observed at Mt. Cimone (2165 m a.s.l.), Italy, during the PEGASOS campaign. *Atmos. Chem. Phys.* **2015**, *15* (19), 11327−11340.
(30) Rosati, B.; Gysel, M.; Rubach, F.; Mentel, T. F.; Goger, B.; Poulain, L.; Schlag, P.; Miettinen, P.; Pajunoja, A.; Virtanen, A.; Klein Baltink, H.; Henzing, J. S. B.; Größ, J.; Gobbi, G. P.; Wiedensohler, A.; Kiendler-Scharr, A.; Decesari, S.; Facchini, M. C.; Weingartner, E.; Baltensperger, U. Vertical profiling of aerosol hygroscopic properties in the planetary boundary layer during the PEGASOS campaigns. *Atmos. Chem. Phys.* **2016**, *16* (11), 7295−7315.
(31) Whiteman, C. D.; Zhong, S.; Shaw, W. J.; Hubbe, J. M.; Bian, X.; Mittelstadt, J. Cold Pools in the Columbia Basin. *Weather and Forecasting* **2001**, *16* (4), 432.
(32) Utah State University. *Cache Valley Air Quality Studies*. http://www.deq.utah.gov/Pollutants/P/pm/pm25/cachevalley/docs/2010/09Sep/CacheValleyAirQualityStudies2006.pdf (assessed May 9, 2017).
(33) Chow, J. C.; Chen, L. W. A.; Watson, J. G.; Lowenthal, D. H.; Magliano, K. A.; Turkiewicz, K.; Lehrman, D. E. PM2.5 chemical composition and spatiotemporal variability during the California Regional PM10/PM2.5 Air Quality Study (CRPAQS); *J. Geophys. Res.: Atmos.*; **2006**, *111*, D10, 10.1029/2005JD006457
(34) Brown, S. G.; Roberts, P. T.; McCarthy, M. C.; Lurmann, F. W.; Hyslop, N. P. Wintertime vertical variations in particulate matter (PM) and precursor concentrations in the San Joaquin Valley during the California Regional Coarse PM/Fine PM Air Quality Study. *J. Air Waste Manage. Assoc.* **2006**, *56* (9), 1267−1277.
(35) Ferrero, L.; Perrone, M. G.; Petraccone, S.; Sangiorgi, G.; Ferrini, B. S.; Lo Porto, C.; Lazzati, Z.; Cocchi, D.; Bruno, F.; Greco, F.; Riccio, A.; Bolzacchini, E. Vertically-resolved particle size distribution within and above the mixing layer over the Milan metropolitan area. *Atmos. Chem. Phys.* **2010**, *10* (8), 3915−3932.
(36) Ferrero, L.; Cappelletti, D.; Moroni, B.; Sangiorgi, G.; Perrone, M. G.; Crocchianti, S.; Bolzacchini, E. Wintertime aerosol dynamics and chemical composition across the mixing layer over basin valleys. *Atmos. Environ.* **2012**, *56*, 143−153.
(37) Ferrero, L.; Castelli, M.; Ferrini, B. S.; Moscatelli, M.; Perrone, M. G.; Sangiorgi, G.; D'Angelo, L.; Rovelli, G.; Moroni, B.; Scardazza, F.; Močnik, G.; Bolzacchini, E.; Petitta, M.; Cappelletti, D. Impact of black carbon aerosol over Italian basin valleys: high- resolution measurements along vertical profiles, radiative forcing and heating rate. *Atmos. Chem. Phys.* **2014**, *14* (18), 9641−9664.
(38) Lurmann, F. W.; Brown, S. G.; McCarthy, M. C.; Roberts, P. T. Processes influencing secondary aerosol formation in the San Joaquin Valley during winter. *J. Air Waste Manage. Assoc.* **2006**, *56* (12), 1679−1693.
(39) Watson, J. G.; Chow, J. C. A wintertime $PM_{2.5}$ episode at the Fresno, CA, supersite. *Atmos. Environ.* **2002**, *36* (3), 465−475.

DOI: 10.1021/acs.est.6b06603
Environ. Sci. Technol. 2017, 51, 5941−5950

(40) Kim, Y. J.; Spak, S. N.; Carmichael, G. R.; Riemer, N.; Stanier, C. O. Modeled aerosol nitrate formation pathways during wintertime in the Great Lakes region of North America. *J. Geophys. Res.: Atmos.* **2014**, *119* (21), 12420−12445.
(41) Stanier, C.; Singh, A.; Adamski, W.; Baek, J.; Caughey, M.; Carmichael, G.; Edgerton, E.; Kenski, D.; Koerber, M.; Oleson, J.; Rohlf, T.; Lee, S. R.; Riemer, N.; Shaw, S.; Sousan, S.; Spak, S. N. Overview of the LADCO winter nitrate study: hourly ammonia, nitric acid and $PM_{2.5}$ composition at an urban and rural site pair during $PM_{2.5}$ episodes in the US Great Lakes region. *Atmos. Chem. Phys.* **2012**, *12* (22), 11037−11056.
(42) Curci, G.; Ferrero, L.; Tuccella, P.; Barnaba, F.; Angelini, F.; Bolzacchini, E.; Carbone, C.; Denier van Der Gon, H. A. C.; Facchini, M. C.; Gobbi, G. P.; Kuenen, J. P. P.; Landi, T. C.; Perrino, C.; Perrone, M. G.; Sangiorgi, G.; Stocchi, P. How much is particulate matter near the ground influenced by upper-level processes within and above the PBL? A summertime case study in Milan (Italy) evidences the distinctive role of nitrate. *Atmos. Chem. Phys.* **2015**, *15* (5), 2629−2649.
(43) Neuman, J. A.; Nowak, J. B.; Brock, C. A.; Trainer, M.; Fehsenfeld, F. C.; Holloway, J. S.; Hübler, G.; Hudson, P. K.; Murphy, D. M.; Nicks, D. K.; Orsini, D.; Parrish, D. D.; Ryerson, T. B.; Sueper, D. T.; Sullivan, A.; Weber, R. Variability in ammonium nitrate formation and nitric acid depletion with altitude and location over California. *J. Geophys. Res.: Atmos.* **2003**, *108* (D17) 10.1029/2003JD003616.
(44) Levy, H. Normal atmosphere: Large radical and formaldehyde concentrations predicted. *Science* **1971**, *173* (3992), 141−143.
(45) Young, C. J.; Washenfelder, R. A.; Roberts, J. M.; Mielke, L. H.; Osthoff, H. D.; Tsai, C.; Pikelnaya, O.; Stutz, J.; Veres, P. R.; Cochran, A. K.; Vandenboer, T. C.; Flynn, J.; Grossberg, N.; Haman, C. L.; Lefer, B.; Stark, H.; Graus, M.; de Gouw, J.; Gilman, J. B.; Kuster, W. C.; Brown, S. S. Vertically resolved measurements of nighttime radical reservoirs in Los Angeles and their contribution to the urban radical budget. *Environ. Sci. Technol.* **2012**, *46* (20), 10965.
(46) Volkamer, R.; Sheehy, P.; Molina, L. T.; Molina, M. J. Oxidative capacity of the Mexico City atmosphere − Part 1: A radical source perspective. *Atmos. Chem. Phys.* **2010**, *10* (14), 6969−6991.
(47) Schnell, R. C.; Oltmans, S. J.; Neely, R. R.; Endres, M. S.; Molenar, J. V.; White, A. B. Rapid photochemical production of ozone at high concentrations in a rural site during winter. *Nat. Geosci.* **2009**, *2* (2), 120−122.

DOI: 10.1021/acs.est.6b06603
Environ. Sci. Technol. 2017, 51, 5941−5950